CNS Neuroscience & Therapeutics

ORIGINAL ARTICLE

CNS Neuroscience & Therapeutics

Atp13a2 Deficiency Aggravates Astrocyte-Mediated Neuroinflammation via NLRP3 Inflammasome Activation

Chen Qiao,[1] Nuo Yin,[1] Huan-Yu Gu,[1] Jia-Lei Zhu,[1] Jian-Hua Ding,[1] Ming Lu[1] & Gang Hu[1,2]

1 Jiangsu Key Laboratory of Neurodegeneration, Department of Pharmacology, Nanjing Medical University, Nanjing, Jiangsu, China
2 Biomedical Functional Materials Collaborative Innovation Center, College of Chemistry and Materials Science, Nanjing Normal University, Nanjing, Jiangsu, China

Keywords
Astrocytes; ATP13A2; Cathepsin B; NLRP3 inflammasome; Parkinson's disease.

Correspondence
Gang Hu, M.D., Ph.D., Jiangsu Key Laboratory of Neurodegeneration, Department of Pharmacology, Nanjing Medical University, 140 Hanzhong Road, Nanjing, Jiangsu 210029, China.
Tel.: +86-25-86863169;
Fax: +86-25-86863108;
E-mail: ghu@njmu.edu.cn
Received 5 November 2015; revision 21 December 2015; accepted 22 December 2015

doi: 10.1111/cns.12514

SUMMARY

Aim: *Atp13a2* (Park9) gene encodes a transmembrane lysosomal P5-type ATPase (ATP13A2), and its missense or truncation mutations leads to lysosomal dysfunction and consequently results in neuronal death in the pathogenesis of Parkinson's disease (PD). Nevertheless, the roles of ATP13A2 in the biological features of astrocytes, especially in the regulation of PD-related neuroinflammation, have not been investigated. **Methods:** We cultured primary neurons and astrocytes from mouse midbrain to investigate the mechanisms for astrocyte ATP13A2-regulated lysosomal function and neuroinflammation following 1-methyl-4-phenylpyridinium (MPP^+) treatment. **Results:** We found that astrocytes expressed considerable levels of ATP13A2 and deficiency of ATP13A2 in astrocyte-induced intense inflammation, which exacerbated dopaminergic neuron damage after exposure to MPP^+. Notably, lack of ATP13A2 increased lysosomal membrane permeabilization and cathepsin B release, which in turn exacerbated activation of nod-like receptor protein 3 (NLRP3) inflammasome to produce excess IL-1β from astrocytes. Furthermore, overexpression of ATP13A2 reversed MPP^+-induced cathepsin B release and NLRP3 inflammasome activation in astrocytes. **Conclusions:** Our results have revealed a novel role of ATP13A2 in modulating astrocyte-mediated neuroinflammation via NLRP3 inflammasome activation, thus bringing to light of a direct link between astrocyte lysosome and neuroinflammation in the pathological model of PD.

Introduction

Parkinson's disease (PD) is a multifactorial disorder, characterized by the deposition of Lewy bodies and loss of dopaminergic neurons in the substantia nigra pars compacta (SNc) [1–3]. The enhanced oxidative stress [4], protein misfolding and aggregation [5], and dysfunction of the ubiquitin–proteasome system [6] are involved in the pathogenesis of PD, but the exact mechanisms that contribute to dopaminergic neuronal degeneration remain unclear. Impairment of lysosome function with aging has been implicated in of the pathological progress of PD [7,8]. For example, the brain samples from postmortem PD patients show decreased lysosomal markers and increased accumulation of autophagosomes [9,10]. Several crucial genes linked to parkinsonian syndromes are also associated with the lysosomal functions, including leucine-rich repeat kinase 2 (*LRRK2*), *SNCA*, *GBA*, *SNCA*, and *Atp13a2* [8,11,12]. Thus, targeting lysosomal function may be a potential strategy for treatment of PD.

On the other, neuroinflammation is a known factor in the pathogenesis of neurodegenerative diseases (multiple sclerosis, Alzheimer's disease, and PD) [3,13]. Recent literature has pointed to the consequence of inflammasome-mediated inflammatory pathways in neuroinflammation [1]. Recently, the role of NLRP3 inflammasomes, in oxidative stress-induced neuroinflammation and impaired amyloid metabolism seen in AD brains, has been evaluated and recognized [14]. Several regulatory mechanisms have been identified to suppress NLRP3 inflammasome. For example, dopamine (DA) has a protective role for MPTP-induced loss of dopaminergic neurons by suppressing NLRP3 inflammasome activation [15]. These aforementioned studies suggest that inflammasome activation may be linked to severity in PD. The dysfunction of lysosomes is involved in the regulation of inflammation, but the direct relation between lysosomes-mediated inflammation and the pathophysiology of PD is still poorly illustrated.

Astrocytes are the most abundant cell type in the brain and play crucial roles in maintaining the brain homeostasis [16]. In particular, astrocytes are important in the development and maintenance of neuronal survival via balancing the release of inflammatory factors and trophic factors [17]. Furthermore, the activated astrocytes are critical for neuroinflammation and influence the survival of dopaminergic neurons [1,18], thereby targeting neuroinflammation could slow down the process of PD. New data have emerged suggesting that inflammasomes control the vital roles in

astrocyte-mediated inflammation. We recently reported that astrocytes are activated in response to 1-methyl-4-phenyl-1, 2, 3, 6-tetrahydropyridine/probenecid (MPTP/p) injury and increase remarkable NLRP3 inflammasome activation, within PD mouse model [19]. However, whether the genes targeting lysosome function participate in the modulation of inflammasomes activation in astrocytes has not been clearly clarified.

Atp13a2 (*Park9*) gene encodes a transmembrane lysosomal P5-type ATPase (ATP13A2), exerting vital physiological function in mammalian cells [20]. ATP13A2 is highly expressed in the brain, including the SNc [21,22], a region that displays progressive degeneration of dopamine neurons in PD. This distribution feature highly suggests that ATP13A2 is involved in the PD pathophysiology. Indeed, missense or truncation mutations in the *Atp13a2* gene impairs lysosomal functions, resulting in an autosomal recessive levodopa-responsive early-onset parkinsonism, known as Kufor–Rakeb syndrome (KRS) [21]. Furthermore, studies have shown that loss of ATP13A2 impairs the stability of the lysosome membrane and suppresses the clearance of substrates in neurons [21]. Nevertheless, the roles of ATP13A2 in the biological features of astrocytes, especially in the regulation of inflammation, remain elusive.

Herein, we revealed a novel role of ATP13A2 in modulating astrocyte-mediated neuroinflammation via NLRP3 inflammasome activation following 1-methyl-4-phenylpyridinium (MPP^+) treatment. Our findings indicate that ATP13A2 represents a potential critical mediator of astrocyte-induced neuroinflammation and a potential therapeutic target of delaying the degeneration of neurons in PD.

Materials and Methods

Animals and Reagents

Atp13a2 KO C57BL/6J mice were donated by Professor Ding-Feng Su (Department of Pharmacology, Second Military Medical University, Shanghai, China). The age-matched littermate WT mice were used as controls. All animals were maintained under specific pathogen-free conditions and treated according to the protocols approved by IACUC (Institutional Animal Care and Use committee of Nanjing Medical University).

Most chemicals and reagents were purchased from Sigma Chemical Co. (St Louis, MO, USA). The reagents obtained from other sources are detailed throughout the following text.

Primary Astrocytic Culture and Transfection

Neonatal mice (age 1–3 days) were sacrificed by rapid decapitation, the midbrain was removed and separated from meninges and basal ganglia, and tissue was dissociated with 0.25% trypase (Amresco, Solon, OH, USA) at 37°C and terminated by Dulbecco's modified Eagle's medium (DMEM, Gibco-BRL, Rockville, MD, USA) supplemented with 10% fetal bovine serum. After centrifugation at 1000 *g* for 5 min, the cell pellets were resuspended and plated on a poly-lysine-treated flask. Culture media were changed 24 h later to complete medium and subsequently twice a week. Cultures were shaken to remove the top layer of cells sitting over the astrocytic monolayer to yield mainly type I astrocytes with a flat morphology between day 5 and 7. Before experimental treatments, astrocytic cultures were shaken for 4 h and passaged once to remove microglia, and then, we use the method of immunofluorescence to identify the purity of astrocytes. The purity of astrocytes was as high as 95%.

ATP13A2-V5 plasmid was obtained from Professor Zhuo-Hua Zhang (State Key Laboratory of Medical Genetics, Xiangya Medical School, Central South University, Changsha, China). Astrocytes were cultured at a confluency of 70–80% in six-well/24-well dishes and transfected with 1 μg or 2 μg of the ATP13A2-V5 cDNA (pcDNA3.1-hATP13A2) [23] or the pcDNA3.1 empty vector and ATP13A2-siRNA or negative control siRNA (100 nM, Santa Cruz) in OptiMEM (Gibco) using Lipofectamine™ 3000 Transfection Reagent (Invitrogen, Carlsbad, CA, USA) for 6 h. For the induction of neurological damage, astrocytes were incubated with ultrapure MPP^+ (50 μM) for 48 h. For pharmacological measurements, the cathepsin B inhibitor (20 μM, Santa Cruz) was added to the cell culture medium 1 h before MPP^+ stimulation. The cell extracts and precipitated supernatants were analyzed by ELISA and Western blotting.

Identification and Quantification of TH Immunoreactivity Neurons and Neuronal Processes

Mesencephalic neurons were performed according to our previously described protocol [24]. After incubation with the collection of astrocytic supernatant for 12 h, cells were rinsed carefully with 0.1 M PBS and fixed with 4% paraformaldehyde (PFA), then followed by immunohistochemistry as described above. The number of TH immunoreactivity (TH-ir) neurons was counted in 10 randomly selected fields on a Nikon Optical TE2000-S inverted microscope. The values were normalized to that obtained from control culture. The average number of TH-ir cells in control cultures ranged from 20 to 30 per field, while TH-ir cells made up about 5% of all cells in primary culture. Each TH-ir cell process was traced from soma to the end of the process, realized by the measurement function of Image Pro Plus 5.1.

Immunofluorescence

Cultured astrocytes were fixed with 4% PFA for 15 min. After rinsing three times with PBS, cells were incubated in 5% BSA (0.3% Triton X-100 in PBS) for 1 h and then incubated with polyclonal rabbit anti-GFAP (1:800; Millipore, Boston, MA, USA) and mouse anti-cathepsin B (1:500; R&D Systems, Minneapolis, CA, USA) at 4°C overnight. Alexa Fluor 555-conjugated donkey anti-rabbit and Alexa Fluor 488-conjugated donkey anti-mouse were purchased from Invitrogen. Photographs were assessed by laser scanning confocal microscopy (Perkin Elmer, Waltham, MA, USA).

Quantitative Real-Time Reverse Transcription–Polymerase Chain Reaction

Total RNA was extracted from cultured cells with Trizol reagent (Invitrogen Life technologies, Carlsbad, CA, USA). Reverse transcription PCR was carried out using a TaKaRa PrimeScript RT

reagent kit, and real-time PCR was measured using a QuantiTect SYBR Green PCR kit (Qiagen) with an ABI 7300 Fast Real-Time PCR System (Applied Biosystems, Foster City, CA, USA). The sequences of primers for real-time PCR analysis are as follows: glyceraldehyde-3-phosphate dehydrogenase (GAPDH) (forward primer 5′-CAAAAGGGTCATCTCC-3′ and reverse primer 5′-CCCCAGCATCAAAGGTG-3′); (ATP13A2 forward primer 5′-ATGCCAGTAGTAGCAAGACAGGTG-3′ and reverse primer 5′-CA GTCTTATCTATGTGGCTTTGGTG-3′); tumor necrosis factor-alpha (TNF-α) (forward 5′-CATCTTCTCAAAATTCGAGTGACAA-3′ and reverse 5′-TGGGAGTAGACAAGGTACAACCC-3′); interleukin-1β (IL-1β) (forward 5′-TCATTGTGGCTGTGGAGAAG-3′ and reverse 5′-AGGCCACAGGTATTTTGT CG-3′); IL-4 (forward 5′-TCGG CATTTTGAACGAGGTC-3′ and reverse 5′-GAAAAGCCCGAAA GAGTCTC-3′); IL-6 (forward 5′-ATCCAGTTGCCTTCTT GGGACT GA-3′ and reverse 5′-TAAGCCTCCGACTTGTGAAGTGGT-3′); IL-10 (forward 5′-TGCTATGCTGCCTGCTCTTA-3′ and reverse 5′-TCATTTCCGATAA GGCTTGG-3′); glial derived neurotrophic factor (GDNF) (forward 5′-GACTTGGGTCTGGGCTATGA-3′ and reverse 5′-ACATGCCTGCCCTACTTTGT-3′); fibroblast growth factor 2 (FGF2) (forward 5′-GGTCACAGCGGCAGATAAAAA GAC-3′ and reverse 5′-TTGGGTAGTTCGGCATTGCGAG-3′). After the addition of primers, and template DNA to the master, PCR thermal cycle parameters were as follows: 95°C for 10 min, 40 cycles of 60°C for 60 s, and 95°C for 15 s, and a melting curve from 60 to 95°C to ensure amplification of a single product. The GAPDH gene was used as an endogenous control to normalize for differences in the amount of total RNA in each sample.

Enzyme-Linked Immunosorbent Assay (ELISA)

Cells were treated with different stimuli (MPP^+ 50 μM for 48 h, LPS 100 ng/mL for 12 h, ATP 5 mM for 30 min, MDP (Invivogen, Santiago, CA, USA) 10 μg/mL for 18 h, flagellin (Invivogen) 10 μg/mL for 12 h, and dsDNA (Invivogen) 2 μg/mL for 48 h). The concentration of IL-1β and TNF-α in the cell culture supernatant was measured by mouse IL-1β ELISA Kit (R&D) and mouse TNF-α ELISA kit (ExCell Bio, Shanghai, China) according to the manufacturer's instructions.

Purification of Cell Culture Supernatant Protein

The cell culture supernatant (SN) was collected, centrifuged to remove dead cells, and the SN was transferred into new tubes. Then, 500 μL methanol and 125 μL chloroform were added to precipitate SN, vortex, and centrifuge 5 min at 16,000 *g*. The upper phase was discarded without touching the proteins disk, and 500 μL methanol was added and centrifuged for 5 min at 16,000 *g* for washing. The SN was removed, and the pellet was dried at 37°C for 5 min. Ultimately, 50 μL 2.5× loading buffer was added with DTT and vortex. The samples were boiled and loaded on 12–15% gels.

Western Blotting Analysis

Midbrain and astrocytes protein lysates were quantified by Bradford assays (Bio-Rad, Hercules, CA, USA). Proteins were electrophoresed through a 10–15% SDS–polyacrylamide gel and blotted to PVDF membrane. Blots were probed with the following primary antibodies: rabbit anti-ATP13A2 (1:1000), mouse anti-cathepsin B (1:1000; R&D), mouse anti-TH (1:5000; Sigma), mouse anti-NLRP3(1:1000; Adipogen, Santiago, CA, USA), rabbit anti-caspase-1 (1:500; Millipore), goat anti-IL-1β (1:500; Sigma), rabbit anti-p-IKKβ/t-IKKβ (1:1000; Cell Signaling Technology, Boston, MA, USA), rabbit anti-p65 (1:1000; Cell Signaling), mouse anti-histone 3 (1:1000; Cell Signaling), and mouse-β-actin (1:1000; Sigma). The blots were incubated with HRP-conjugated secondary antibodies and signals detected by enhanced chemiluminescence (ECL) Western blot detection reagents (Pierce, Rockford, IL, USA). The membranes were scanned and analyzed using an Image Quant LAS 4000 Chemiluminescence Imaging System (GE Healthcare, Stockholm, Sweden).

Statistics

Results were analyzed using GraphPad Prism 5.0. Data were first examined for equal variance and then subjected to two-way repeated-measures ANOVA with time and genotype as variables, with Bonferroni's *post hoc* tests at treatment. Student's *t*-tests were used for single variant analyses. In all studies, n indicates the number of samples per group, and a critical value of $P \leq 0.05$ was used. Data are plotted as means ± SEM.

Results

Lack of ATP13A2 Induces Astrocytic Inflammation and Exacerbates TH^+ Neuronal Damage

MPTP, a component in some insecticides, is one of the most used molecules to model neurodegenerative diseases, in particular Parkinson's disease [25]. MPTP is oxidized in glial cells, mainly in astrocytes, throughout the action of monoamine oxidase B into MPP^+, which is further incorporated to the dopaminergic neurons where it impairs mitochondrial function, induces inflammation [19]. Thus, we selected MPP^+ to treat cultured mesencephalic astrocytes model for the mechanisms study in PD. Before addressing the role of ATP13A2 in regulating the biological features of astrocytes following MPP^+ treatment, we first observed *Atp13a2* gene and protein expression in mesencephalic astrocytes. As expected, *Atp13a2* mRNA and ATP13A2 protein were detected in primary cultured mesencephalic astrocytes using RT-PCR (Figure 1A, upper) and Western blot (Figure 1A, lower). We further found the protein of ATP13A2 was 53% down-regulated by suffering from 50 μM MPP^+ stimulation for 48 h in astrocytes (*t*-test, $P = 0.01$) (Figure 1B), suggesting the involvement of ATP13A2 in this model.

To explore the role of ATP13A2 in regulating astrocyte response to MPP^+, we utilized astrocytes from wild-type (WT) mouse and *Atp13a2* knockout (KO) mouse (Figure S1). After treated with 50 μM MPP^+ for 48 h, astrocytes increased the generation of pro-inflammatory cytokines, including tumor necrosis factor-α (TNF-α) (two-way ANOVA, MPP^+: $F_{1,12} = 11.546$, $P = 0.005$; genotype: $F_{1,12} = 165.005$, $P < 0.001$; interaction: $F_{1,12} = 1.538$, $P = 0.239$) and interleukin-6 (IL-6) (two-way ANOVA, MPP^+: $F_{1,12} = 20.346$, $P < 0.001$; genotype: $F_{1,12} = 63.730$, $P < 0.001$; interaction:

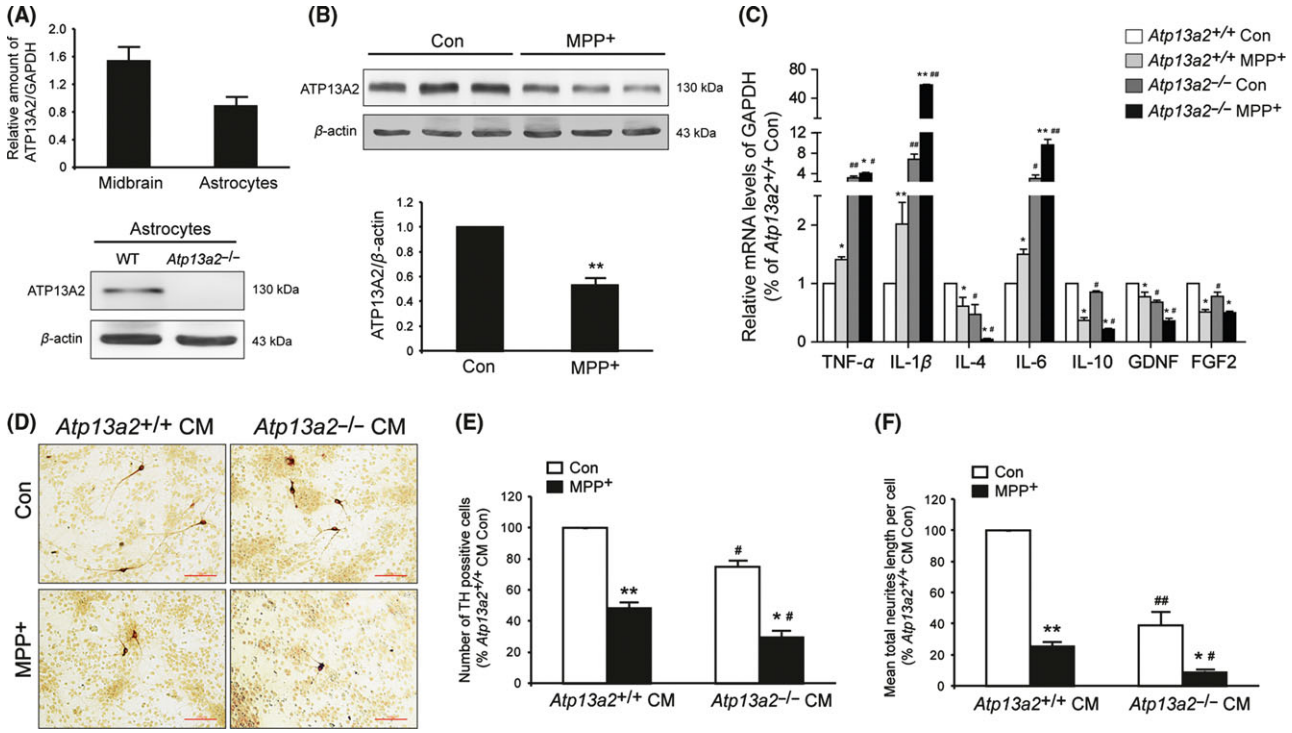

Figure 1 *Atp13a2* knockout increased inflammatory cytokine release in astrocytes and exacerbated TH^+ neuron damage induced by MPP^+. (**A**) The results of real-time PCR showed that the *Atp13a2 gene* was expressed in the midbrain tissue as well as cultured astrocytes (upper). Western blot results showed that astrocytes from WT mice, but not from Atp13a2 KO mice, expressed ATP13A2 (lower) (from four independent experiments). (**B**) Representative immunoblots and densitometry analysis demonstrated that MPP^+ treatment downregulated ATP13A2 expression in mesencephalic astrocytes (from six independent experiments). Data are presented as mean ± SEM, $^{**}P < 0.01$ versus control group. (**C**) The mRNA of inflammatory cytokines and nutritional factors detected by RT-PCR (from six independent experiments). Data are presented as mean ± SEM, two-way ANOVA, $^{*}P < 0.05$, $^{**}P < 0.01$ versus control group in corresponding genotype; $^{\#}P < 0.05$, $^{\#\#}P < 0.01$ versus corresponding *Atp13a2*$^{+/+}$ groups. (**D**) After astrocytic conditioned medium (CM) stimulating primary cultured neurons of midbrain 6 h, TH immunohistochemistry detected the dopaminergic neurons. (**E** and **F**) Representative the number of TH-positive cells and neurite length compared with WT control (from four independent experiments). Data are presented as mean ± SEM, two-way ANOVA, $^{*}P < 0.05$, $^{**}P < 0.01$ versus control group in corresponding genotype; $^{\#}P < 0.05$, $^{\#\#}P < 0.01$ versus corresponding *Atp13a2*$^{+/+}$ CM groups (**H**).

$F_{1,12} = 22.355$, $P < 0.001$), but decreased the production of anti-inflammatory cytokines, such as IL-4 (two-way ANOVA, MPP^+: $F_{1,12} = 13.451$, $P = 0.003$; genotype: $F_{1,12} = 24.112$, $P < 0.001$; interaction: $F_{1,12} = 0.036$, $P = 0.853$) and IL-10 (two-way ANOVA, MPP^+: $F_{1,12} = 342.912$, $P < 0.001$; genotype: $F_{1,12} = 19.382$, $P = 0.001$; interaction: $F_{1,12} = 0.009$, $P = 0.926$). Observably, the lack of ATP13A2 exacerbated MPP^+-induced the release of proinflammatory cytokine and decreased the anti-inflammatory cytokine compared with WT MPP^+ groups. Notably, *Atp13a2* knockout significantly raised the mRNA level of IL-1β by 8.5-fold of WT control groups in astrocytes at baseline (two-way ANOVA, MPP^+: $F_{1,12} = 1540.147$, $P < 0.001$; genotype: $F_{1,12} = 2149.906$, $P < 0.001$; interaction: $F_{1,12} = 1423.853$, $P < 0.001$. Compared with respective Con groups, MPP^+ increased the mRNA level of IL-1β by 2.0-fold in WT mice, but increased the mRNA level of IL-1β by 8.0-fold in KO mice, and there was a meaningful rate of change between KO and WT treatment groups) (Figure 1C). In addition, *Atp13a2* knockout markedly exacerbated MPP^+-induced down-regulation of neurotrophic factors, including glial cell line-derived neurotrophic factor (GDNF) (two-way ANOVA, MPP^+: $F_{1,12} = 21.896$, $P = 0.001$; genotype: $F_{1,12} = 41.229$, $P < 0.001$; interaction: $F_{1,12} = 0.264$, $P = 0.617$. Compared with respective Con groups, MPP^+ decreased the mRNA level of GDNF by 20% in WT mice, but decreased the mRNA level of GDNF by 55% in KO mice, and there was a meaningful rate of change between KO and WT treatment groups) and fibroblast growth factor 2 (FGF2) (two-way ANOVA, MPP^+: $F_{1,12} = 34.248$, $P < 0.001$; genotype: $F_{1,12} = 6.230$, $P = 0.028$; interaction: $F_{1,12} = 3.904$, $P = 0.072$. *Atp13a2* knockout significantly decreased the mRNA level of FGF2 by 20% in WT mice without MPP^+ stimulation; nevertheless, compared with respective Con groups, MPP^+ decreased the mRNA level of FGF2 by 50% in WT mice, but decreased the mRNA level of FGF2 by 38% in KO mice, and the rate of change from MPP^+ to Con groups in WT astrocytes was higher than KO astrocytes.) (Figure 1C).

It is known that the release of inflammatory cytokines and neurotrophic factors from astrocytes contributes to neuronal growth and survival [17]. To identify the effect of altered astrocyte reactivation caused by ATP13A2 deficiency in dopaminergic cell fate after MPP^+ treatment, we collected the supernatant of astrocytes

both in normal and MPP^+-treatment conditions to stimulate primary cultured mesencephalic neurons from WT pregnant mice. The tyrosine hydroxylase (TH) immunohistochemical staining was used to evaluate the survival of dopaminergic neurons. Interestingly, even without MPP^+ stimulation, the supernatant of *Atp13a2*-null astrocytes decreased 25% TH-ir neurons (two-way ANOVA, MPP^+: $F_{1,12} = 385.061$, $P < 0.001$; genotype: $F_{1,12} = 78.782$, $P < 0.001$; interaction: $F_{1,12} = 1.536$, $P = 0.239$) and shorten 60% neurite length (two-way ANOVA, MPP^+: $F_{1,12} = 555.243$, $P < 0.001$; genotype: $F_{1,12} = 308{,}023$, $P < 0.001$; interaction: $F_{1,12} = 98.745$, $P < 0.001$) compared with WT astrocytes (Figure 2C–E). Moreover, exposure to the conditioned medium of MPP^+-treated KO astrocytes further exacerbated damage of TH-ir neurons. Because of the significant differences between WT and KO groups at baseline, the rate of change from MPP^+ to Con groups in WT astrocytes was higher than KO astrocytes. Thus, *Atp13a2* knockout induces reactive astrocyte-mediated neuronal damage, especially exacerbates the degeneration of DA neurons. Taken together, the above results demonstrate that *Atp13a2* deficiency in astrocytes improves MPP^+-induced inflammatory cytokine production and down-regulation of neurotrophic factors, which subsequently impairs dopaminergic neuronal survival in the baseline condition as well as following MPP^+ treatment.

Downregulation of Atp13a2 Activates NLRP3 Inflammasome in Astrocytes

Among the secreted factors, the levels of IL-1β exerted the most change in *Atp13a2* KO astrocytes in response to MPP^+ stimulation (Figure 1C). IL-1β promotes a number of innate immune processes associated with infection, inflammation, and autoimmunity, thereby responsible for neuroinflammation and associated brain diseases in the central nervous system (CNS)

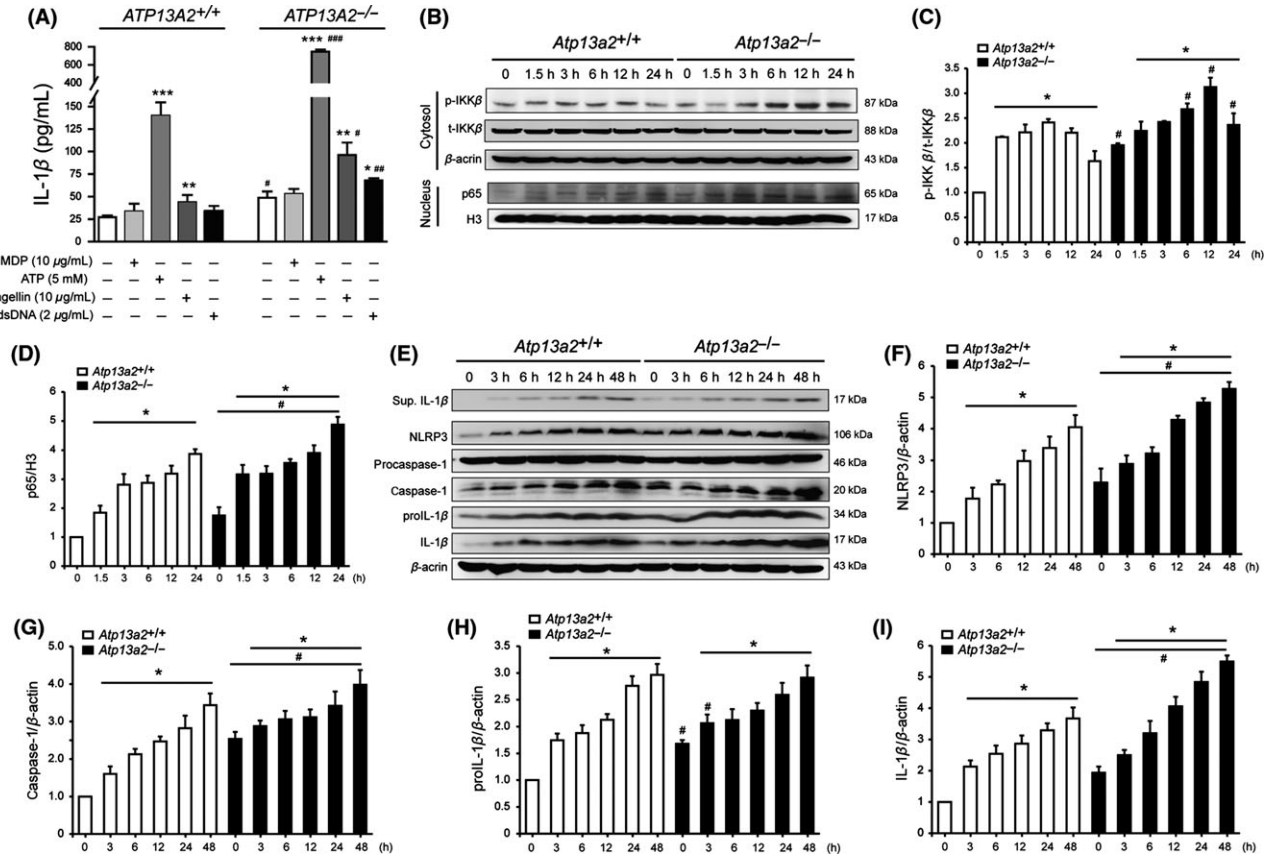

Figure 2 *Atp13a2* knockout stimulated MPP^+-induced NLRP3 inflammasome activation in astrocytes. (**A**) Astrocytes were treated with different inflammasome activator to induce the specific inflammasome activation. IL-1β from astrocytic supernatant was detected by ELISA. NLRP1 inflammasome: transfected MDP 10 μg/mL for 18 h; NLRP3 inflammasome: ATP 5 mM for 30 min; NLRC4 inflammasome: flagellin 10 μg/mL for 12 h; AIM2 inflammasome: transfected dsDNA 2 μg/mL for 48 h. All the stimulations were pre-incubated with LPS (100 ng/mL) for 12 h, (from six independent experiments). Data are presented as mean SEM from at least six independent experiments. Two-way ANOVA, $^*P < 0.05$, $^{**}P < 0.01$, $^{***}P < 0.001$ versus control group in corresponding genotype; $^{\#}P < 0.05$, $^{\#\#}P < 0.01$, $^{\#\#\#}P < 0.001$ versus corresponding *Atp13a2*$^{+/+}$ groups. (**B**) To examine the time point of the effects of ATP13A2 on MPP^+-induced activation of first signal to produces pro-IL-1β by Western blotting, we detected p-IKKβ and nucleus-p65 (from three independent experiments). (**C** and **D**) The analysis of p65 and p-IKKβ, respectively. (**E**) Along with the time of MPP^+ stimulation, the activation of second signal was responsible for the activation of NLRP3, caspase-1, and mature IL-1β, (from three independent experiments). (**F**–**I**) The analysis of NLRP3, caspase-1, proIL-1β, and IL-1β, respectively. Data are presented as mean $\pm$ SEM from at least four independent experiments. Two-way ANOVA, $^*P < 0.05$ versus control group in corresponding genotype; $^{\#}P < 0.05$ versus corresponding *Atp13a2*$^{+/+}$ groups at the same time point.

[13,26]. There is increasing evidence that the production and secretion of IL-1β are involved in inflammasome activation [27]. Different inflammasomes, such as NLRP1, NLRP3, NLRC4, and AIM2, exert various functions in different types of brain cells including astrocytes [27]. Thus, we treated cultured WT and KO astrocytes with different activators of specific inflammasome and detected the release of IL-1β by ELISA. Surprisingly, we found that the recognized activator of NLRP3 inflammasome, and lipopolysaccharide (LPS) with adenosine triphosphate (ATP) significantly increased IL-1β release in KO astrocytes compared with WT controls (Figure 2A). Muramyl dipeptide (MDP), an activator of NLRP1 inflammasome, did not induce the secretion of IL-1β in both genotype astrocytes. In addition, the NLRC4 inflammasome activator flagellin and the AIM2 inflammasome activator dsDNA promoted the release of IL-1β from astrocytes, which was more aggravated in KO astrocytes. But it should be emphasized that the activation of NLRP3 inflammasome was the most prominent compared with other inflammasomes (Figure 2A). In summary, we demonstrate that ATP13A2 is involved in mediating NLRP3 inflammsome in astrocytes to induce inflammation.

Evidence indicates that most, if not all, of the activation of NLRP3 inflammasome requires two signals: "signal 1," priming signal to generate pro-IL-1β via the activation of NF-κB pathway, and "signal 2," mature signal to convert pro-IL-1β into the activated IL-1β induced by caspase-1 cleavaged under the activation of NLRP3 inflammasome [27]. To clarify the effect of ATP13A2 on NLRP3 inflammasome activation in astrocytes, we firstly detected the time course of inflammatory responses in both WT and KO astrocytes treated with or without MPP^+. We found phosphorylation levels of IKKβ were increased within 12 h under MPP^+ treatment, which gradually reduced over time. But the nucleus translocation of p65 was increased continuously (Figure 2B–D). Next, we collected the cell extracts after MPP^+-triggered 12 h to examine the activation of "signal 1" to produce pro-IL-1β. The expression levels of those components of inflammasome, such as NLRP3, caspase-1, proIL-1β, and IL-1β, were upregulated in a time-dependent manner (Figure 2F–I). In particular, the upregulation of IL-1β secretion in astrocytic supernatant also followed in a time-dependent manner. In the following study, we utilized MPP^+ to stimulate astrocytes for 48 h in order to detect mature NLRP3 inflammasome.

To confirm the function of ATP13A2 in NLRP3 inflammasome activation of astrocytes and eliminate the effects of gene knockout itself, we further utilized a small interfering RNA (siRNA) transduction system to knockdown ATP13A2 in WT astrocytes. Using this approach, ~68% reduction of ATP13A2 expression was achieved compared with scrambled shRNA control (*t*-test, $P < 0.05$) (Figure S2A). Consistently, silencing of ATP13A2 in astrocytes resulted in NLRP3 inflammasome activation compared with those in control shRNA-treated astrocytes (Figure 3A) (two-way ANOVA, MPP^+: $F_{1,12} = 63.481$, $P = 0.001$; genotype [shRNA]: $F_{1,12} = 7.427$, $P = 0.018$; interaction: $F_{1,12} = 1.477$, $P = 0.248$). Moreover, Western blot analysis revealed an apparent upregulation of inflammasome components under MPP^+ stimulation within 48 h, including the expression of NLRP3 (Figure 3A, B) (two-way ANOVA, MPP^+: $F_{1,12} = 4.085$, $P = 0.066$; genotype [shRNA]: $F_{1,12} = 5.516$, $P = 0.037$; interaction: $F_{1,12} = 0.319$, $P = 0.583$), caspase-1 (Figure 3C) (two-way ANOVA, MPP^+: $F_{1,12} = 0.269$, $P = 0.028$; genotype [shRNA]: $F_{1,12} = 1.125$, $P = 0.310$; interaction: $F_{1,12} = 0.005$, $P = 0.944$), proIL-1β (Figure 3D) and the release of IL-1β (two-way ANOVA, MPP^+: $F_{1,12} = 5.216$, $P = 0.041$; genotype [shRNA]: $F_{1,12} = 11.977$, $P = 0.005$; interaction: $F_{1,12} = 0.198$, $P = 0.664$) (Figure 3E). However, as a result of the obviously changes at baseline between the genotypes, the rate of change from MPP^+ to Con groups in Con-siR astrocytes was close to the changes in ATP13A2-siR astrocytes. Together, these results demonstrate that the deficiency of ATP13A2 results in NLRP3 inflammasome activation in mesencephalic astrocytes.

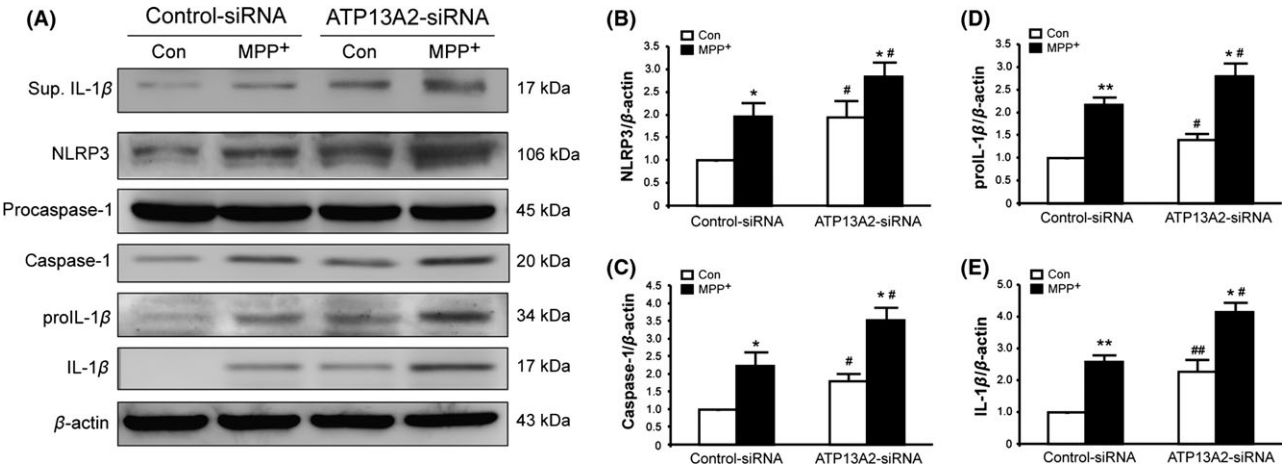

Figure 3 ATP13A2 knockdown aggravated MPP^+-induced NLRP3 inflammasome activation in astrocytes. (**A**) Silencing of ATP13A2 in WT primary astrocytes by siRNA, we evaluated the expression of NLRP3 inflammasome components by Western blotting. (**B**–**E**) Representative quantification for analysis of cathepsin B, NLRP3, caspase-1, pro-IL-1β, and IL-1β (cytoplasm and supernatant) expression in astrocytes. Data are presented as mean ± SEM from at least four independent experiments, two-way ANOVA, $^*P < 0.05$, $^{**}P < 0.01$ versus control group in corresponding siRNA groups; $^{\#}P < 0.05$, $^{\#\#}P < 0.01$ versus corresponding control siRNA groups.

Release of Lysosomal Cathepsin B Contributes to *Atp13a2* Deficiency-Induced NLRP3 Inflammasome Activation in Astrocytes

Cathepsin B is a lysosomal cysteine protease primarily involved in the degradation or processing of lysosomal proteins [28], under certain conditions, the secretion of cathepsin B binds to NLRP3 and rapidly induced inflammasomes activation [29]. To determine the potential mechanisms underlying *Atp13a2* deficiency-mediated inflammation, we examined the expression of cathepsin B in the astrocytes of both genotypes under MPP^+ treatment in a time-dependent manner. We found that the expression of cathepsin B was upregulation by MPP^+ challenge in a time-dependent manner, and *Atp13a2* knockout remarkably increased lysosomal cathepsin B expression (Figure 4A), suggesting that silencing of ATP13A2 expression would induced the lysosomal proteolytic enzyme outflow and impaired lysosomal function. Nevertheless, the rate of change from MPP^+ to Con groups in WT astrocytes had no significant differences compared with the rate in KO astrocytes (Figure 4A, lower). The laser confocal microscopy further revealed that *Atp13a2* knockout dramatically increased the expression of cathepsin B in glial fibrillary acidic protein (GFAP)-positive cells at baseline, the GFAP was marked with astrocytes (Figure 4B). To determine the effect of cathepsin B on *Atp13a2*-ablation-induced inflammsome activation, astrocytes were pretreated with cathepsin B specific inhibitor Z-FA-FMK before MPP^+ challenge. NLRP3-dependent caspase-1 activation (two-way ANOVA, MPP^+: $F_{3,24} = 19.121$, $P < 0.001$; genotype: $F_{1,24} = 14.235$, $P = 0.001$; interaction: $F_{3,24} = 2.181$, $P = 0.116$) and IL-1β maturation (two-way ANOVA, MPP^+: $F_{3,24} = 28.023$, $P < 0.001$; genotype: $F_{1,24} = 28.207$, $P < 0.001$; interaction: $F_{3,24} = 2.935$, $P = 0.054$) by MPP^+ or *Atp13a2* deficiency were indeed inhibited by cathepsin B inhibitor (Figure 4D–F). These results indicate that *Atp13a2* knockout increases astrocytic cathepsin B expression and subsequently activates NLRP3 inflammasome, thereby enhances the secretion of astrocyte-derived pro-inflammatory cytokines.

Overexpression of ATP13A2 Decreases the Release of Cathepsin B and Attenuates NLRP3 Inflammasome Activation in Astrocytes

The impaired integrity of the lysosomal membrane was a crucial factor to aggravate astrocytic inflammation. To identify whether ATP13A2 is responsible for the activation of NLRP3 inflamma-

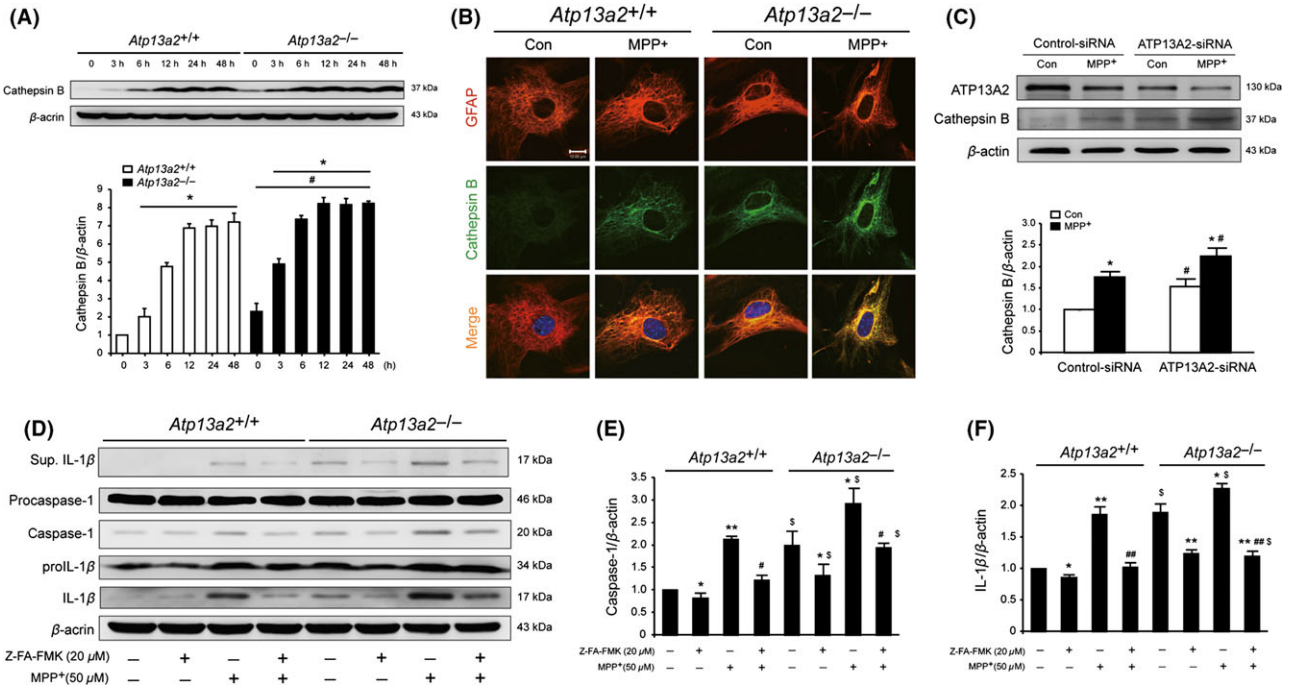

Figure 4 ATP13A2 decreased the release of cathepsin B and inhibits NLRP3 inflammasome activation. (**A**) Along with the time of MPP^+ stimulation, the injury lysosome increased the expression of cathepsin B by Western blot. Data are presented as mean ± SEM from at least four independent experiments. Two-way ANOVA, $^*P < 0.05$ versus control group in corresponding genotype; $^{\#}P < 0.05$ versus corresponding $Atp13a2^{+/+}$ groups at the same time point. (**B**) Double immunofluorescence of GFAP (red) and cathepsin B (green), DAPI stains nucleus (blue), it was detected by laser confocal microscopy. (**C**) Silencing of ATP13A2 in WT primary astrocytes by siRNA, we evaluated the expression of ATP13A2 and cathepsin B by Western blot. Data are presented as mean ± SEM from at least four independent experiments, two-way ANOVA, $^*P < 0.05$ versus control group in corresponding siRNA groups; $^{\#}P < 0.05$ versus corresponding control siRNA groups. (**D**) Before MPP^+-triggered 48 h, preincubation of cathepsin B inhibitor for 1 h, then detected the expression of caspase-1 and IL-1β in cells extracts by Western blot. (**E** and **F**) The analysis of the expression of cleaved caspase-1 and mature IL-1β, respectively (from four independent experiments). Data are presented as mean ± SEM, two-way ANOVA, $^*P < 0.05$, $^{**}P < 0.01$ versus control group in corresponding genotype; $^{\#}P < 0.05$, $^{\#\#}P < 0.01$ versus MPP^+ group in corresponding genotype; $^{\$}P < 0.05$ versus corresponding $Atp13a2^{+/+}$ groups.

some induced by cathepsin B outflow, we used ATP13A2-V5 plasmid to transfect both genotypic astrocytes. Transfection efficiency was shown in Figure S2B. Most notably, overexpression of ATP13A2 dramatically reduced the expression of cathepsin B (two-way ANOVA, MPP^+: $F_{3,24} = 35.115$, $P < 0.001$; genotype [overexpression]: $F_{1,24} = 31.617$, $P < 0.001$; interaction: $F_{3,24} = 4.536$, $P = 0.012$) (Figure 5A). In particular, we discovered that MPP^+ could significantly increase both genotype astrocytes secreting mature IL-1β, while overexpression of ATP13A2 decreased the release of IL-1β (Figure 5B) in both genotypes with or without MPP^+ treatment. The ELISA results of TNF-α revealed the same tendency with IL-1β (Figure S3). The reduced release of IL-1β reminders the suppression of inflammasome and the change of TNF-α suggests the inhibition of NF-κB signaling pathway. To further confirm this, we tested the "signaling pathway" of NLRP3 inflammasome activation. The results showed that overexpression of ATP13A2 markedly alleviated MPP^+-induced activation of NF-κB signaling pathway in astrocytes. Moreover, it reduced the expression of p65 and the phosphorylation levels of IKKβ (two-way ANOVA, MPP^+: $F_{3,24} = 11.277$, $P < 0.001$; genotype [overexpression]: $F_{1,24} = 30.228$, $P < 0.001$; interaction: $F_{3,24} = 2.875$, $P = 0.057$) in *Atp13a2* knockout astrocytes in the presence or absence of MPP^+ treatment (Figure 5C–E). Furthermore, overexpression of ATP13A2 plasmid effectively suppressed caspase-1 activation (two-way ANOVA, MPP^+: $F_{3,24} = 110.282$, $P < 0.001$; genotype [overexpression]: $F_{1,24} = 82.147$, $P < 0.001$; interaction: $F_{3,24} = 20.592$, $P < 0.001$) and subsequent IL-1β production and secretion (two-way ANOVA, MPP^+: $F_{3,24} = 263.551$, $P < 0.001$; genotype [overexpression]: $F_{1,24} = 51.062$, $P < 0.001$; interaction: $F_{3,24} = 22.677$, $P < 0.001$) induced by MPP^+, which was accompanied by the decrease of NLRP3 inflammasome activation in *Atp13a2* deficiency astrocytes (Figure 5F–I). Together, these results illustrate that ATP13A2 inhibits astrocyte-mediated inflammation via suppressing NF-κB translocation and NLRP3 inflammasome activation.

Discussion

Mutations of *Atp13a2* have been associated with an autosomal recessive levodopa-responsive early-onset parkinsonism [21]. Increasing evidence suggests that ATP13A2 is a potential therapeutic target for PD [12,30]. Previous studies showed that loss of ATP13A2 disrupts the function of lysosomes and aggravates neuronal impairment [22]. Astrocytes, the most abundant cell types in the brain, are responsible for neuroinflammation regulation and nutrition support [31]; nevertheless, the roles of ATP13A2 in astrocyte biological features are not well known. In the present study, we showed that mouse astrocytes express ATP13A2 protein and deficiency of ATP13A2 in astrocytes increase the vulnerability of DA neuron in response to MPP^+ challenge. This finding is consistent with our recent *in vivo* studies that *Atp13a2* knockout aggravated overactivation of astrocytes in the SNc of MPTP/p PD mice, accompanied by intense neuroinflammation (unpublished data). Furthermore, *Atp13a2* knockout in astrocytes exacerbates

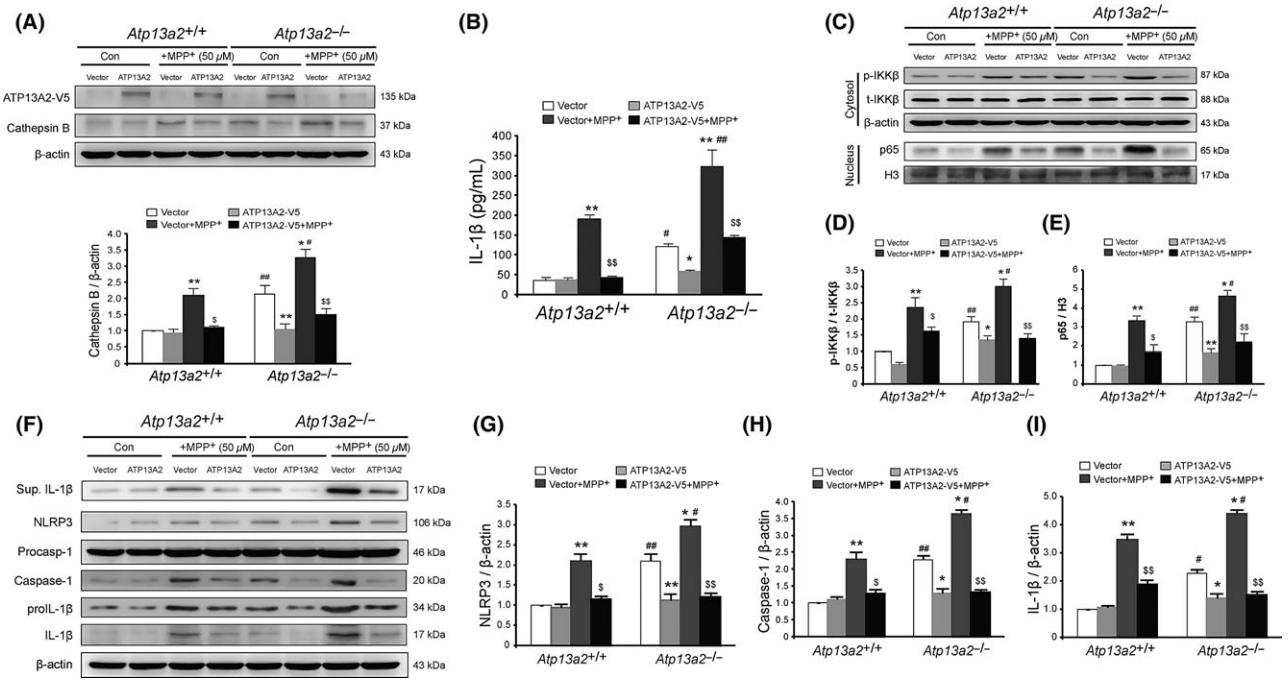

Figure 5 Overexpression of ATP13A2 inhibited the secretion of cathepsin B and NLRP3 inflammasome activation in primary astrocytes. (**A**) Representative immunoblots and quantification for analysis cathepsin B expression after transfection of ATP13A2 plasmid in astrocytes. (**B**) The secretion of IL-1β from astrocytic supernatant was detected by ELISA (from eight independent experiments). (**C**–**E**) Overexpression of ATP13A2 decreased the expression of nucleus-p65 and phosphorylation levels of IKKβ in WT and KO astrocytes with or without MPP^+ treatment (from four independent experiments). (**F**–**I**) The expression of NLRP3, caspase-1, and IL-1β was examined by Western blotting. Data are presented as mean ± SEM from at least four independent experiments. Two-way ANOVA, $^*P < 0.05$, $^{**}P < 0.01$ versus control group in corresponding genotype; $^{\#}P < 0.05$, $^{\#\#}P < 0.01$ versus MPP^+ group in corresponding genotype; $^{\$}P < 0.05$, $^{\$\$}P < 0.01$ versus corresponding *Atp13a2*$^{+/+}$ groups.

lysosome membrane damage and cathepsin B release, which in turn, markedly improves the activation of NLRP3 inflammasome. Most notably, overexpression of ATP13A2 inhibits NLRP3 inflammasome-mediated inflammation in astrocytes. Taken together, our study reveals a novel role of ATP13A2 in the communication between lysosome and neuroinflammation in astrocytes.

Growing evidence indicates that ATP13A2 may have a profound role in maintaining the stability of the lysosome membrane structure and promoting the clearance of misfolded proteins, thereby regulating the neuronal integrity [22]. Lysosomes also exert a far-reaching influence on astrocytes, not only on neurons [32]. Astrocytes cannot be just identified as "brain glue," but rather they respond to activation and have active modulatory roles in intercellular communication to maintain neuronal activity and survival [33]. Recent studies have suggested the proliferation and activation of astrocytes could be an "alarm bell" during neurodegeneration, especially in astrocyte-mediated inflammation [34]. In the model of MPP^+ stimulation, the protein of ATP13A2 expression is significantly decreased, which could be portentous of great change. Remarkably, *Atp13a2* knockout strengthens the activation of NLRP3 inflammasome and accelerates the secretion of mature IL-1β in astrocytes, revealing that astrocytic ATP13A2 has the ability to adjust the neuroinflammation, including in PD. Furthermore, the secretions from astrocytes lacking *Atp13a2* trigger the loss of DA neurons with or without MPP^+ stimulation. These results further support the review that ATP13A2 is a novel therapeutic target of PD. Because microglia also play an important role in neuroinflammation of PD [35,36], in the future study, we will examine whether ATP13A2 is also involved in microglia-mediated inflammation.

The *Atp13a2* gene encodes a lysosomal type 5 P-type ATPase. Several groups have found that loss of ATP13A2 function results in impaired lysosomal function and, consequently, accumulation of misfolded proteins and neurotoxicity in neurons. However, the roles of ATP13A2 in astrocytes have not been studied. In the present study, we found that activated astrocytes produce a large number of inflammatory cytokines that contribute to the loss function of ATP13A2. Among these inflammatory cues, IL-1β is the most significant substrates. As we known, IL-1β has been recognized to be essential for initiation and progress of PD [37,38]. IL-1β production is dependent on NLRP3 inflammasome activation: a primary signal that activates NF-κB pathway to induce pro-IL-1β and NLRP3 synthesis and a secondary signal that activates the inflammasome and the subsequent caspase-1 processing [27]. In the present study, we found that *Atp13a2* knockout in cultured mesencephalic astrocytes markedly increases the activation of NF-κB and NLRP3 inflammasome expression following the stimulation of MPP^+. These findings indicate that deficiency of ATP13A2 results in overactivation of the NLRP3 inflammasome following MPP^+ treatment, playing a crucial role in the pathological model of PD.

Cysteine cathepsins comprise 11 members denoted by letters: cathepsins B, C, F, H, K, L, V, O, S, W, and Z. Emerging data have shown that cathepsin B enhances the aggregate forming activity of α-synuclein fibrils and is involved in the process of PD [39]. Furthermore, cathepsin B properly regulates the degradation of protein [40] and strongly activates the NLRP3 inflammasome in response to stress [29]. In this study, we found that *Atp13a2* knockout increases cathepsin B release from lysosome, and the oversecretion of cathepsin B further activates the NLRP3 inflammasome. As a specific inhibitor of cathepsin B, Z-FA-FMK is capable of alleviating the activity of caspase-1 and IL-1β due to the deficiency of ATP13A2 or MPP^+ stimulation. These results suggest that *Atp13a2* knockout most likely trigger the release of cathepsin B to adjust and control NLRP3 inflammasome activation, in turn, to modify astrocytic inflammation. Future work should examine how other cathepsins are involved in the ATP13A2-mediated astrocytic function.

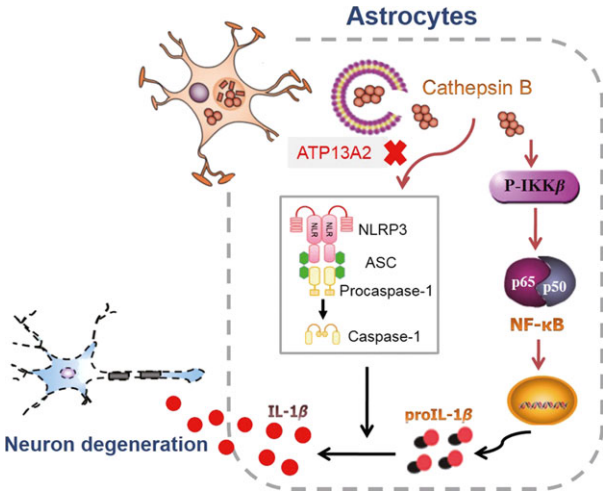

Figure 6 Astrocytic ATP13A2 inhibits NLRP3 inflammasome activation in astrocytes. The loss function of ATP13A2 lead to lysosomal membrane rupture, which resulted in cathepsins B overflowed in astrocytes. The release of cathepsin B activates the NLRP3 inflammasome and aggravates DA neurons degeneration.

In the present study, we used the primary astrocytes and MPTP/MPP^+ model to study the potential impact of ATP13A2 on astrocytes. Knockdown or knockout the expression of ATP13A2 on astrocytes could accelerate the astrocytic inflammation. Notably, we found that *Atp13a2* knockout significantly aggravated astrocytic activation and proliferation in response to MPTP administration (unpublished data). Our future project is to establish $Atp13a2^{hGFAP}$ conditional knockout mice to further elucidate the potential contribution of astrocyte *Atp13a2* in PD pathogenesis.

Conclusions

We demonstrated for the first time that ATP13A2 modulates astrocyte-mediated neuroinflammation via NLRP3 inflammasome activation (Figure 6). Our study reveals a novel role of ATP13A2 in astrocytes and brings to light a direct link between lysosome and neuroinflammation in the pathological model of PD, suggesting that ATP13A2 might be a promising therapeutic target for PD and other lysosomal storage diseases.

Acknowledgments

We thank Professor Ding-Feng Su (Second Military Medical University) for providing $Atp13a2^{-/-}$ mice and Professor Zhuo-Hua Zhang (Central South University) for providing ATP13A2-V5

plasmid. We thank Professor Ming Xiao (Nanjing Medical University) and Ming Li (Nebraska–Lincoln University) for help with revising the manuscript. The work reported herein was supported by the grants from the National Natural Science Foundation of China (Nos 81473196, 81202514, and 81573403), the National Science & Technology Major Project (No. 2012ZX09304-001), the Natural Science Foundation of Jiangsu Province (BK20130039), and the key project of Natural Science Foundation of the Higher Education Institutions of Jiangsu Province (No. 15KJA310002).

Conflict of Interests

The authors declare no conflict of interest.

References

1. Wang Q, Liu Y, Zhou J. Neuroinflammation in Parkinson's disease and its potential as therapeutic target. *Transl Neurodegener* 2015;**4**:19.
2. He Y. Imaging brain networks in neurodegenerative diseases. *CNS Neurosci Ther* 2015;**21**:751–753.
3. Baggio HC, Segura B, Junque C. Resting-state functional brain networks in Parkinson's disease. *CNS Neurosci Ther* 2015;**21**:793–801.
4. Katunina EA, Titova NV, Malykhina EA, et al. Oxidative stress and Parkinson's disease: mechanisms and perspectives of treatment. *Zh Nevrol Psikhiatr Im S S Korsakova* 2015;**115**:141–145.
5. Paleologou KE, El-Agnaf OM. alpha-Synuclein aggregation and modulating factors. *Subcell Biochem* 2012;**65**:109–164.
6. Opattova A, Cente M, Novak M, Filipcik P. The ubiquitin proteasome system as a potential therapeutic target for treatment of neurodegenerative diseases. *Gen Physiol Biophys* 2015. [Epub ahead of print].
7. Platt FM, Boland B, van der Spoel AC. The cell biology of disease: lysosomal storage disorders: the cellular impact of lysosomal dysfunction. *J Cell Biol* 2012;**199**:723–734.
8. Manzoni C, Lewis PA. Dysfunction of the autophagy/lysosomal degradation pathway is a shared feature of the genetic synucleinopathies. *FASEB J* 2013;**27**:3424–3429.
9. Dehay B, Bove J, Rodriguez-Muela N, et al. Pathogenic lysosomal depletion in Parkinson's disease. *J Neurosci* 2010;**30**:12535–12544.
10. Chu Y, Dodiya H, Aebischer P, Olanow CW, Kordower JH. Alterations in lysosomal and proteasomal markers in Parkinson's disease: relationship to alpha-synuclein inclusions. *Neurobiol Dis* 2009;**35**:385–398.
11. Mills RD, Mulhern TD, Cheng HC, Culvenor JG. Analysis of LRRK2 accessory repeat domains: prediction of repeat length, number and sites of Parkinson's disease mutations. *Biochem Soc Trans* 2012;**40**:1086–1089.
12. Holemans T, Sorensen DM, van Veen S, et al. A lipid switch unlocks Parkinson's disease-associated ATP13A2. *Proc Natl Acad Sci U S A* 2015;**112**:9040–9045.
13. Singhal G, Jaehne EJ, Corrigan F, Toben C, Baune BT. Inflammasomes in neuroinflammation and changes in brain function: a focused review. *Front Neurosci* 2014;**8**:315.
14. Shi JQ, Zhang CC, Sun XL, et al. Antimalarial drug artemisinin extenuates amyloidogenesis and neuroinflammation in APPswe/PS1dE9 transgenic mice via inhibition of nuclear factor-kappaB and NLRP3 inflammasome activation. *CNS Neurosci Ther* 2013;**19**:262–268.
15. Yan Y, Jiang W, Liu L, et al. Dopamine controls systemic inflammation through inhibition of NLRP3 inflammasome. *Cell* 2015;**160**:62–73.
16. Bayraktar OA, Fuentealba LC, Alvarez-Buylla A, Rowitch DH. Astrocyte development and heterogeneity. *Cold Spring Harb Perspect Biol* 2014;**7**:a020362.
17. Cabezas R, Avila M, Gonzalez J, et al. Astrocytic modulation of blood brain barrier: perspectives on Parkinson's disease. *Front Cell Neurosci* 2014;**8**:211.
18. Efremova L, Schildknecht S, Adam M, et al. Prevention of the degeneration of human dopaminergic neurons in an astrocyte co-culture system allowing endogenous drug metabolism. *Br J Pharmacol* 2015;**172**:4119–4132.
19. Lu M, Sun XL, Qiao C, Liu Y, Ding JH, Hu G. Uncoupling protein 2 deficiency aggravates astrocytic endoplasmic reticulum stress and nod-like receptor protein 3 inflammasome activation. *Neurobiol Aging* 2014;**35**:421–430.
20. De La Hera DP, Corradi GR, Adamo HP, De Tezanos Pinto F. Parkinson's disease-associated human P5B-ATPase ATP13A2 increases spermidine uptake. *Biochem J* 2013;**450**:47–53.
21. Ramirez A, Heimbach A, Grundemann J, et al. Hereditary parkinsonism with dementia is caused by mutations in ATP13A2, encoding a lysosomal type 5 P-type ATPase. *Nat Genet* 2006;**38**:1184–1191.
22. Usenovic M, Tresse E, Mazzulli JR, Taylor JP, Krainc D. Deficiency of ATP13A2 leads to lysosomal dysfunction, alpha-synuclein accumulation, and neurotoxicity. *J Neurosci* 2012;**32**:4240–4246.
23. Tan J, Zhang T, Jiang L, et al. Regulation of intracellular manganese homeostasis by Kufor–Rakeb syndrome-associated ATP13A2 protein. *J Biol Chem* 2011;**286**:29654–29662.
24. Xie J, Duan L, Qian X, Huang X, Ding J, Hu G. K(ATP) channel openers protect mesencephalic neurons against MPP+-induced cytotoxicity via inhibition of ROS production. *J Neurosci Res* 2010;**88**:428–437.
25. Przedborski S, Vila M. The 1-methyl-4-phenyl-1,2,3,6-tetrahydropyridine mouse model: a tool to explore the pathogenesis of Parkinson's disease. *Ann N Y Acad Sci* 2003;**991**:189–198.
26. Tao AF, Xu ZH, Chen B, et al. The pro-inflammatory cytokine interleukin-1beta is a key regulatory factor for the postictal suppression in mice. *CNS Neurosci Ther* 2015;**21**:642–650.
27. de Rivero Vaccari JP, Dietrich WD, Keane RW. Therapeutics targeting the inflammasome after central nervous system injury. *Transl Res* 2016;**167**:35–45.
28. Li S, Du L, Zhang L, et al. Cathepsin B contributes to autophagy-related 7 (Atg7)-induced nod-like receptor 3 (NLRP3)-dependent proinflammatory response and aggravates lipotoxicity in rat insulinoma cell line. *J Biol Chem* 2013;**288**:30094–30104.
29. Bruchard M, Mignot G, Derangere V, et al. Chemotherapy-triggered cathepsin B release in myeloid-derived suppressor cells activates the Nlrp3 inflammasome and promotes tumor growth. *Nat Med* 2013;**19**:57–64.
30. Rochet JC. New insights into lysosomal dysfunction in Parkinson's disease: an emerging role for ATP13A2. *Mov Disord* 1092;**2012**:27.
31. Perea G, Sur M, Araque A. Neuron-glia networks: integral gear of brain function. *Front Cell Neurosci* 2014;**8**:378.
32. Xu M, Yang L, Rong JG, et al. Inhibition of cysteine cathepsin B and L activation in astrocytes contributes to neuroprotection against cerebral ischemia via blocking the tBid-mitochondrial apoptotic signaling pathway. *Glia* 2014;**62**:855–880.
33. Baxter P. Astrocytes: more than just glue. *Dev Med Child Neurol* 2012;**54**:291.
34. Halliday GM, Stevens CH. Glia: initiators and progressors of pathology in Parkinson's disease. *Mov Disord* 2011;**26**:6–17.
35. Tufekci KU, Meuwissen R, Genc S, Genc K. Inflammation in Parkinson's disease. *Adv Protein Chem Struct Biol* 2012;**88**:69–132.
36. Kim JY, Kim N, Yenari MA. Mechanisms and potential therapeutic applications of microglial activation after brain injury. *CNS Neurosci Ther* 2015;**21**:309–319.
37. Koprich JB, Reske-Nielsen C, Mithal P, Isacson O. Neuroinflammation mediated by IL-1beta increases susceptibility of dopamine neurons to degeneration in an animal model of Parkinson's disease. *J Neuroinflammation* 2008;**5**:8.
38. Walsh S, Gavin A, Wyatt S, et al. Knockdown of interleukin-1 receptor 1 is not neuroprotective in the 6-hydroxydopamine striatal lesion rat model of Parkinson's disease. *Int J Neurosci* 2015;**125**:70–77.
39. Tsujimura A, Taguchi K, Watanabe Y, et al. Lysosomal enzyme cathepsin B enhances the aggregate forming activity of exogenous alpha-synuclein fibrils. *Neurobiol Dis* 2015;**73**:244–253.
40. Fonovic M, Turk B. Cysteine cathepsins and extracellular matrix degradation. *Biochim Biophys Acta* 2014;**1840**:2560–2570.

Supporting Information

The following supplementary material is available for this article:

Figure S1. Gene identification for *Atp13a2* knockout mice.
Figure S2. The transfection efficiency on astrocytes.
Figure S3. Overexpression of ATP13A2 inhibited MPP^+-induced the release of TNF-α from astrocytes.

